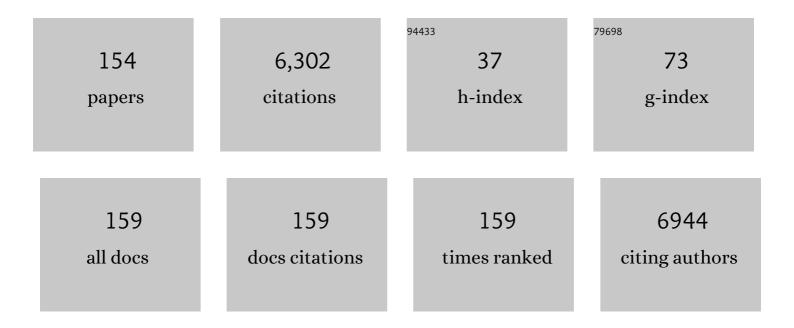
List of Publications by Year in descending order

Source: https://exaly.com/author-pdf/7075272/publications.pdf Version: 2024-02-01



Ρινοκιίν Υλν

#	Article	IF	CITATIONS
1	Finite element modeling with subjectâ€specific mechanical properties to assess knee osteoarthritis initiation and progression. Journal of Orthopaedic Research, 2023, 41, 72-83.	2.3	2
2	Deep neural networks for the assessment of surgical skills: A systematic review. Journal of Defense Modeling and Simulation, 2022, 19, 159-171.	1.7	19
3	OASIS: One-pass aligned atlas set for medical image segmentation. Neurocomputing, 2022, 470, 130-138.	5.9	10
4	On a Sparse Shortcut Topology of Artificial Neural Networks. IEEE Transactions on Artificial Intelligence, 2022, 3, 595-608.	4.7	6
5	Shadow-Consistent Semi-Supervised Learning for Prostate Ultrasound Segmentation. IEEE Transactions on Medical Imaging, 2022, 41, 1331-1345.	8.9	28
6	Deep learning for biomechanical modeling of facial tissue deformation in orthognathic surgical planning. International Journal of Computer Assisted Radiology and Surgery, 2022, 17, 945-952.	2.8	11
7	Polar transform network for prostate ultrasound segmentation with uncertainty estimation. Medical Image Analysis, 2022, 78, 102418.	11.6	13
8	Deep learning-based motion artifact removal in functional near-infrared spectroscopy. Neurophotonics, 2022, 9, 041406.	3.3	10
9	Transformed Grid Distance Loss forÂSupervised Image Registration. Lecture Notes in Computer Science, 2022, , 177-181.	1.3	1
10	Functional Brain Imaging Reliably Predicts Bimanual Motor Skill Performance in a Standardized Surgical Task. IEEE Transactions on Biomedical Engineering, 2021, 68, 2058-2066.	4.2	17
11	Multi-Task Learning for Registering Images With Large Deformation. IEEE Journal of Biomedical and Health Informatics, 2021, 25, 1624-1633.	6.3	9
12	Integrative analysis for COVID-19 patient outcome prediction. Medical Image Analysis, 2021, 67, 101844.	11.6	57
13	Prediction of Coronary Calcification and Stenosis: Role of Radiomics From Low-Dose CT. Academic Radiology, 2021, 28, 972-979.	2.5	9
14	Biomedical imaging and analysis through deep learning. , 2021, , 49-74.		2
15	Cross-Modal Attention for MRI and Ultrasound Volume Registration. Lecture Notes in Computer Science, 2021, , 66-75.	1.3	29
16	Task-Oriented Low-Dose CT Image Denoising. Lecture Notes in Computer Science, 2021, , 441-450.	1.3	6
17	Cardiovascular Disease Risk Improves COVID-19 Patient Outcome Prediction. Lecture Notes in Computer Science, 2021, , 467-476.	1.3	0
18	Decreasing the Surgical Errors by Neurostimulation of Primary Motor Cortex and the Associated Brain Activation via Neuroimaging. Frontiers in Neuroscience, 2021, 15, 651192.	2.8	15

#	Article	IF	CITATIONS
19	Transducer Adaptive Ultrasound Volume Reconstruction. , 2021, , .		2
20	Data Augmentation for Training Deep Neural Networks. , 2021, , 151-164.		1
21	Deep learning predicts cardiovascular disease risks from lung cancer screening low dose computed tomography. Nature Communications, 2021, 12, 2963.	12.8	43
22	Association of AI quantified COVID-19 chest CT and patient outcome. International Journal of Computer Assisted Radiology and Surgery, 2021, 16, 435-445.	2.8	21
23	End-to-end Ultrasound Frame to Volume Registration. Lecture Notes in Computer Science, 2021, , 56-65.	1.3	8
24	T <sub>2</sub> Mapping Refined Finite Element Modeling to Predict Knee Osteoarthritis Progression. , 2021, 2021, 4592-4595.		3
25	Knowledge-Based Analysis for Mortality Prediction From CT Images. IEEE Journal of Biomedical and Health Informatics, 2020, 24, 457-464.	6.3	23
26	Boundary-Weighted Domain Adaptive Neural Network for Prostate MR Image Segmentation. IEEE Transactions on Medical Imaging, 2020, 39, 753-763.	8.9	135
27	Deep adaptive registration of multi-modal prostate images. Computerized Medical Imaging and Graphics, 2020, 84, 101769.	5.8	24
28	A method of rapid quantification of patientâ€specific organ doses for CT using deepâ€learningâ€based multiâ€organ segmentation and GPUâ€accelerated Monte Carlo dose computing. Medical Physics, 2020, 47, 2526-2536.	3.0	49
29	Multi-Organ Segmentation Over Partially Labeled Datasets With Multi-Scale Feature Abstraction. IEEE Transactions on Medical Imaging, 2020, 39, 3619-3629.	8.9	101
30	Deep learning in medical image registration: a survey. Machine Vision and Applications, 2020, 31, 1.	2.7	343
31	Synergizing medical imaging and radiotherapy with deep learning. Machine Learning: Science and Technology, 2020, 1, 021001.	5.0	24
32	Deep learning-based liver segmentation for fusion-guided intervention. International Journal of Computer Assisted Radiology and Surgery, 2020, 15, 963-972.	2.8	20
33	Sensorless Freehand 3D Ultrasound Reconstruction via Deep Contextual Learning. Lecture Notes in Computer Science, 2020, , 463-472.	1.3	30
34	High compression deep learning based single-pixel hyperspectral macroscopic fluorescence lifetime imaging in vivo. Biomedical Optics Express, 2020, 11, 5401.	2.9	23
35	Unsupervised Domain Adaptation with Dual-Scheme Fusion Network for Medical Image Segmentation. , 2020, , .		16
36	Division and Fusion: Rethink Convolutional Kernels for 3D Medical Image Segmentation. Lecture Notes in Computer Science, 2020, , 160-169.	1.3	0

Ρινςκών Υάν

4

#	Article	IF	CITATIONS
37	MR Image Super-Resolution via Wide Residual Networks With Fixed Skip Connection. IEEE Journal of Biomedical and Health Informatics, 2019, 23, 1129-1140.	6.3	81
38	Feature Fusion Encoder Decoder Network for Automatic Liver Lesion Segmentation. , 2019, , .		45
39	Fast fit-free analysis of fluorescence lifetime imaging via deep learning. Proceedings of the National Academy of Sciences of the United States of America, 2019, 116, 24019-24030.	7.1	100
40	PASiam: Predicting Attention Inspired Siamese Network, for Space-Borne Satellite Video Tracking. , 2019, , .		15
41	Net-FLICS: fast quantitative wide-field fluorescence lifetime imaging with compressed sensing – a deep learning approach. Light: Science and Applications, 2019, 8, 26.	16.6	64
42	Deep neural maps for unsupervised visualization of high-grade cancer in prostate biopsies. International Journal of Computer Assisted Radiology and Surgery, 2019, 14, 1009-1016.	2.8	17
43	Learning deep similarity metric for 3D MR–TRUS image registration. International Journal of Computer Assisted Radiology and Surgery, 2019, 14, 417-425.	2.8	101
44	fNIRS as a Quantitative tool to Asses and Predict Surgical Skills. , 2019, , .		1
45	A shell and kernel descriptor based joint deep learning model for predicting breast lesion malignancy. , 2019, , .		1
46	Investigation of Physical Phenomena Underlying Temporal-Enhanced Ultrasound as a New Diagnostic Imaging Technique: Theory and Simulations. IEEE Transactions on Ultrasonics, Ferroelectrics, and Frequency Control, 2018, 65, 400-410.	3.0	16
47	Low-Dose CT Image Denoising Using a Generative Adversarial Network With Wasserstein Distance and Perceptual Loss. IEEE Transactions on Medical Imaging, 2018, 37, 1348-1357.	8.9	983
48	Toward a real-time system for temporal enhanced ultrasound-guided prostate biopsy. International Journal of Computer Assisted Radiology and Surgery, 2018, 13, 1201-1209.	2.8	8
49	Correlation-Based Tracking of Multiple Targets With Hierarchical Layered Structure. IEEE Transactions on Cybernetics, 2018, 48, 90-102.	9.5	24
50	Shape prior constrained PSO model for bladder wall MRI segmentation. Neurocomputing, 2018, 294, 19-28.	5.9	20
51	Learning from Noisy Label Statistics: Detecting High Grade Prostate Cancer in Ultrasound Guided Biopsy. Lecture Notes in Computer Science, 2018, , 21-29.	1.3	7
52	A Deep Learning Health Data Analysis Approach: Automatic 3D Prostate MR Segmentation with Densely-Connected Volumetric ConvNets. , 2018, , .		13
53	Adversarial Image Registration with Application for MR and TRUS Image Fusion. Lecture Notes in Computer Science, 2018, , 197-204.	1.3	54

54 Deep compressive macroscopic fluorescence lifetime imaging. , 2018, , .

4

Ρινςκύν Υάν

#	Article	IF	CITATIONS
55	Exploiting Interslice Correlation for MRI Prostate Image Segmentation, from Recursive Neural Networks Aspect. Complexity, 2018, 2018, 1-10.	1.6	37
56	Deep Recurrent Neural Networks for Prostate Cancer Detection: Analysis of Temporal Enhanced Ultrasound. IEEE Transactions on Medical Imaging, 2018, 37, 2695-2703.	8.9	57
57	Transfer learning from RF to B-mode temporal enhanced ultrasound features for prostate cancer detection. International Journal of Computer Assisted Radiology and Surgery, 2017, 12, 1111-1121.	2.8	25
58	Detection and grading of prostate cancer using temporal enhanced ultrasound: combining deep neural networks and tissue mimicking simulations. International Journal of Computer Assisted Radiology and Surgery, 2017, 12, 1293-1305.	2.8	36
59	Tissue mimicking simulations for temporal enhanced ultrasound-based tissue typing. Proceedings of SPIE, 2017, , .	0.8	2
60	Changes in prostate cancer detection rate of MRI-TRUS fusion vs systematic biopsy over time: evidence of a learning curve. Prostate Cancer and Prostatic Diseases, 2017, 20, 436-441.	3.9	52
61	Deeply-supervised CNN for prostate segmentation. , 2017, , .		117
62	MP20-16 TRAINING AND SKILLS ASSESSMENT FOR FUSION-GUIDED PROSTATE BIOPSY: DEFINING THE LEARNING CURVE. Journal of Urology, 2016, 195, .	0.4	2
63	Classifying Cancer Grades Using Temporal Ultrasound for Transrectal Prostate Biopsy. Lecture Notes in Computer Science, 2016, , 653-661.	1.3	7
64	Monitoring of radiofrequency ablation with shear wave delay mapping. , 2015, , .		2
65	ls Visual Registration Equivalent to Semiautomated Registration in Prostate Biopsy?. BioMed Research International, 2015, 2015, 1-7.	1.9	22
66	Label Image Constrained Multiatlas Selection. IEEE Transactions on Cybernetics, 2015, 45, 1158-1168.	9.5	18
67	Machine learning in medical imaging. Computerized Medical Imaging and Graphics, 2015, 41, 1-2.	5.8	27
68	Surface-based registration of liver in ultrasound and CT. Proceedings of SPIE, 2015, , .	0.8	0
69	The Role of Image Guided Biopsy Targeting in Patients with Atypical Small Acinar Proliferation. Journal of Urology, 2015, 193, 473-478.	0.4	30
70	Partial sparse shape constrained sector-driven bladder wall segmentation. Machine Vision and Applications, 2015, 26, 593-606.	2.7	9
71	Multiparametric magnetic resonance imaging-transrectal ultrasound fusion–assisted biopsy for the diagnosis of local recurrence after radical prostatectomy. Urologic Oncology: Seminars and Original Investigations, 2015, 33, 425.e1-425.e6.	1.6	32
72	Feature competition and partial sparse shape modeling for cardiac image sequences segmentation. Neurocomputing, 2015, 149, 904-913.	5.9	20

Ρινςκύν Υάν

#	Article	IF	CITATIONS
73	Pylon line spatial correlation assisted transmission line detection. IEEE Transactions on Aerospace and Electronic Systems, 2014, 50, 2890-2905.	4.7	38
74	Adaptive Shape Prior Constrained Level Sets for Bladder MR Image Segmentation. IEEE Journal of Biomedical and Health Informatics, 2014, 18, 1707-1716.	6.3	48
75	Alternatively Constrained Dictionary Learning For Image Superresolution. IEEE Transactions on Cybernetics, 2014, 44, 366-377.	9.5	81
76	Ego motion guided particle filter for vehicle tracking in airborne videos. Neurocomputing, 2014, 124, 168-177.	5.9	27
77	Object-aware power line detection using color and near-infrared images. IEEE Transactions on Aerospace and Electronic Systems, 2014, 50, 1374-1389.	4.7	27
78	Hierarchical incorporation of shape and shape dynamics for flying bird detection. Neurocomputing, 2014, 131, 179-190.	5.9	16
79	Prostate Biopsy for the Interventional Radiologist. Journal of Vascular and Interventional Radiology, 2014, 25, 675-684.	0.5	15
80	Guest Editorial: Special issue on advanced computing for image-guided intervention. Neurocomputing, 2014, 144, 1-2.	5.9	0
81	Ultrasound-Based Predication of Prostate Cancer in MRI-guided Biopsy. Lecture Notes in Computer Science, 2014, , 142-150.	1.3	3
82	Transfer learning for pedestrian detection. Neurocomputing, 2013, 100, 51-57.	5.9	44
83	Machine learning in medical imaging. Machine Vision and Applications, 2013, 24, 1327-1329.	2.7	6
84	Image registration by normalized mapping. Neurocomputing, 2013, 101, 181-189.	5.9	16
85	Visual Saliency by Selective Contrast. IEEE Transactions on Circuits and Systems for Video Technology, 2013, 23, 1150-1155.	8.3	74
86	Saliency Detection by Multiple-Instance Learning. IEEE Transactions on Cybernetics, 2013, 43, 660-672.	9.5	163
87	Pedestrian detection in unseen scenes by dynamically updating visual words. Neurocomputing, 2013, 119, 232-242.	5.9	3
88	SIFT on manifold: An intrinsic description. Neurocomputing, 2013, 113, 227-233.	5.9	11
89	Robust visual tracking with discriminative sparse learning. Pattern Recognition, 2013, 46, 1762-1771.	8.1	70
90	Greedy regression in sparse coding space for single-image super-resolution. Journal of Visual Communication and Image Representation, 2013, 24, 148-159.	2.8	79

#	Article	IF	CITATIONS
91	Tracking vehicles as groups in airborne videos. Neurocomputing, 2013, 99, 38-45.	5.9	10
92	Learning Saliency by MRF and Differential Threshold. IEEE Transactions on Cybernetics, 2013, 43, 2032-2043.	9.5	26
93	Sparse coding for image denoising using spike and slab prior. Neurocomputing, 2013, 106, 12-20.	5.9	35
94	Manifold Regularized Sparse NMF for Hyperspectral Unmixing. IEEE Transactions on Geoscience and Remote Sensing, 2013, 51, 2815-2826.	6.3	322
95	Global structure constrained local shape prior estimation for medical image segmentation. Computer Vision and Image Understanding, 2013, 117, 1017-1026.	4.7	21
96	Prostate Segmentation in MR Images Using Discriminant Boundary Features. IEEE Transactions on Biomedical Engineering, 2013, 60, 479-488.	4.2	29
97	Multi-spectral saliency detection. Pattern Recognition Letters, 2013, 34, 34-41.	4.2	70
98	Image Super-Resolution Via Double Sparsity Regularized Manifold Learning. IEEE Transactions on Circuits and Systems for Video Technology, 2013, 23, 2022-2033.	8.3	71
99	Machine Learning in Medical Imaging. International Journal of Biomedical Imaging, 2012, 2012, 1-2.	3.9	13
100	Coupled Directional Level Set for MR Image Segmentation. , 2012, , .		6
101	Multi-atlas Based Image Selection with Label Image Constraint. , 2012, , .		5
102	Selecting Key Poses on Manifold for Pairwise Action Recognition. IEEE Transactions on Industrial Informatics, 2012, 8, 168-177.	11.3	43
103	Robust Alternative Minimization for Matrix Completion. IEEE Transactions on Systems, Man, and Cybernetics, 2012, 42, 939-949.	5.0	34
104	Ageâ€related changes in prostate zonal volumes as measured by highâ€resolution magnetic resonance imaging (MRI): a crossâ€sectional study in over 500 patients. BJU International, 2012, 110, 1642-1647.	2.5	45
105	Vehicle detection and tracking in airborne videos by multi-motion layer analysis. Machine Vision and Applications, 2012, 23, 921-935.	2.7	40
106	Geometry constrained sparse coding for single image super-resolution. , 2012, , .		29
107	Confidence guided enhancing brain tumor segmentation in multi-parametric MRI. , 2012, , .		12
108	Visual Attention Accelerated Vehicle Detection in Low-Altitude Airborne Video of Urban Environment. IEEE Transactions on Circuits and Systems for Video Technology, 2012, 22, 366-378.	8.3	14

Ρινςκών Υάν

12

2 62
62
15
0
87
113
75
408
7
21
95
0
2
0
12
6
7

126 Estimating patient-specific shape prior for medical image segmentation. , 2011, , .

#	Article	IF	CITATIONS
127	Local learning-based image super-resolution. , 2011, , .		9
128	Local semi-supervised regression for single-image super-resolution. , 2011, , .		7
129	Learning shape statistics for hierarchical 3D medical image segmentation. , 2011, , .		0
130	Segmenting Images by Combining Selected Atlases on Manifold. Lecture Notes in Computer Science, 2011, 14, 272-279.	1.3	30
131	Collaborative Kalman filters for vehicle tracking. , 2011, , .		2
132	Target-oriented shape modeling with structure constraint for image segmentation. , 2011, , .		0
133	Local adaptive dictionary based image denoising. , 2011, , .		0
134	Image Denoising via Improved Sparse Coding. , 2011, , .		5
135	Medical Image Segmentation Using Descriptive Image Features. , 2011, , .		9
136	Discrete Deformable Model Guided by Partial Active Shape Model for TRUS Image Segmentation. IEEE Transactions on Biomedical Engineering, 2010, 57, 1158-1166.	4.2	100
137	Segmenting TRUS video sequences using local shape statistics. , 2010, , .		2
138	Multi-parametric MRI-pathologic correlation of prostate cancer using tracked biopsies. , 2010, , .		0
139	Incremental Shape Statistics Learning for Prostate Tracking in TRUS. Lecture Notes in Computer Science, 2010, 13, 42-49.	1.3	6
140	Modeling Interaction for Segmentation of Neighboring Structures. IEEE Transactions on Information Technology in Biomedicine, 2009, 13, 252-262.	3.2	11
141	Optimal search guided by partial active shape model for prostate segmentation in TRUS images. , 2009, , ·		7
142	Automatic Segmentation of High-Throughput RNAi Fluorescent Cellular Images. IEEE Transactions on Information Technology in Biomedicine, 2008, 12, 109-117.	3.2	137
143	Learning 4D action feature models for arbitrary view action recognition. , 2008, , .		41
144	Action recognition using spatio-temporal regularity based features. Proceedings of the IEEE International Conference on Acoustics, Speech, and Signal Processing, 2008, , .	1.8	8

#	Article	IF	CITATIONS
145	3D Model based Object Class Detection in An Arbitrary View. , 2007, , .		61
146	A Homographic Framework for the Fusion of Multi-view Silhouettes. , 2007, , .		34
147	Spatio–Temporal Regularity Flow (SPREF): Its Estimation and Applications. IEEE Transactions on Circuits and Systems for Video Technology, 2007, 17, 584-589.	8.3	18
148	Segmentation of volumetric MRA images by using capillary active contour. Medical Image Analysis, 2006, 10, 317-329.	11.6	75
149	Medical Image Segmentation Using Minimal Path Deformable Models With Implicit Shape Priors. IEEE Transactions on Information Technology in Biomedicine, 2006, 10, 677-684.	3.2	31
150	Motion Compensated Lossy-to-Lossless Compression of 4-D Medical Images Using Integer Wavelet Transforms. IEEE Transactions on Information Technology in Biomedicine, 2005, 9, 132-138.	3.2	29
151	Segmentation of Neighboring Organs in Medical Image with Model Competition. Lecture Notes in Computer Science, 2005, 8, 270-277.	1.3	11
152	MRA Image Segmentation with Capillary Active Contour. Lecture Notes in Computer Science, 2005, 8, 51-58.	1.3	17
153	Medical image segmentation with minimal path deformable models. , 0, , .		8
154	Segmentation of Neighboring Structures by Modeling Their Interaction. , 0, , .		0